ResearchGate

See discussions, stats, and author profiles for this publication at: https://www.researchgate.net/publication/6251249

Identification of Anomeric Configuration of Underivatized Reducing Glucopyranosyl-glucose Disaccharides by Tandem Mass Spectrometry and Multivariate Analysis

ARTICLE *in* ANALYTICAL CHEMISTRY · SEPTEMBER 2007

Impact Factor: 5.64 · DOI: 10.1021/ac070317i · Source: PubMed

CITATIONS
33

READS
51

6 AUTHORS, INCLUDING:

Pedro Domingues
University of Aveiro
161 PUBLICATIONS **2,453** CITATIONS
SEE PROFILE

Ana Reis
University of Aveiro
66 PUBLICATIONS **1,056** CITATIONS
SEE PROFILE

Fernando M. Nunes
Universidade de Trás-os-Montes e Alto Douro
91 PUBLICATIONS **988** CITATIONS
SEE PROFILE

M Rosario Domingues
University of Aveiro
228 PUBLICATIONS **2,515** CITATIONS
SEE PROFILE

Available from: Ana Reis
Retrieved on: 31 January 2016

Anal. Chem. **2007,** *79,* 5896−5905

Identification of Anomeric Configuration of Underivatized Reducing Glucopyranosyl-glucose Disaccharides by Tandem Mass Spectrometry and Multivariate Analysis

Joana Simões,[†] Pedro Domingues,[†] Ana Reis,[†] Fernando M. Nunes,[‡] Manuel A. Coimbra,[†] and M. Rosário M. Domingues*,[†]

Department of Chemistry, University of Aveiro, P-3810-193 Aveiro, Portugal, and Department of Chemistry, University of Trás-os-Montes e Alto Douro, P-5000-911 Vila Real, Portugal

The possibility of discrimination of the anomeric configuration (α or *β*) of underivatized reducing glucopyranosyl-glucose disaccharides, using a hybrid mass spectrometer Q-TOF 2 (Micromass), a linear ion trap LXQ (Thermo), and a triple quadrupole Quattro (Micromass) with an electrospray source (ESI) was investigated. Differences observed in the relative abundances of specific product ions obtained from collisionally induced dissociation of the $[M + Li]^+$ adducts were statistically analyzed, and discriminant analysis was performed. MANOVA has shown that anomeric configuration has influence on the combined dependent variables (relative abundances of *m/z* product ions) in all the three mass spectrometers used (Q-TOF 2, LIT, and QqQ). Discriminant analysis has shown that, in all instruments, it is possible to discriminate anomeric configurations and to build a diagnostic model. These diagnostic differences are even more relevant considering that no derivatization procedures are needed for obtaining this structural information. The Q-TOF 2 instrument has been shown to give data that allowed us to build a model with better discriminant power (Wilks' *λ* value of 0.014) followed by the QqQ instrument (Wilks' *λ* value of 0.029) and the LIT instrument (Wilks' *λ* value of 0.037).

Carbohydrates are widely distributed in nature, being responsible for different functions in almost all living organisms. They are present in the living systems as single sugars or associated in polysaccharides, glycoproteins, glycolipids, and others. Their biological activity is dependent on their detailed structure, namely, its composition in monosaccharides, type of linkages, branching, and anomeric configurations. In the past decade, mass spectrometry (MS) has become widely used in the study of carbohydrates due to the development of the soft ionization methods, matrix-assisted laser desorption/ionization[1,2] and electrospray ionization (ESI).[3] Tandem mass spectrometry (MS/MS) proved to be a valuable tool in the structural characterization of carbohydrates, allowing one to obtain detailed information about their structure.[4−6] This approach has the advantage over the other common used methods, such as methylation analysis (GC/MS) and NMR, due to its feasibility even on complex and in trace amounts of samples.[7,8]

Carbohydrate structural characterization by MS/MS is focused on the identification of monomer composition, sequence, and type of linkage in both, derivatized and underivatized oligomers.[1−6,9,10] However, the work devoted to the identification of their anomeric configuration is scarce and is mainly focused on derivatized samples, namely, acetylated xylobiose,[11] benzyl and alkyl hexosyl−fucose disaccharides,[12] and alkyl glucosyl disaccharides.[13,14] Although the conversion of glycans to hydrophobic derivatives, in particular permethylated derivatives allows easy cleanup by organic solvent extraction[15] and enhances the signal intensity,[3] derivatization procedures, however, have the drawback of requiring higher sample amounts as well as the need for cleanup steps prior to their structural characterization. Underivatized glucosyl-glucose disaccharides have been only differentiated, considering

* To whom correspondence should be addressed. E-mail: mrd@dq.ua.pt. Phone: +351 234 370 698. Fax: + 351 234 370 084.

[†] University of Aveiro.

[‡] University of Trás-os-Montes e Alto Douro.

(1) Harvey, D. J. *Mass Spectrom. Rev.* **1999**, *18*, 349−450.
(2) Park, Y.; Lebrilla, C. B. *Mass Spectrom. Rev.* **2005**, *24*, 232−264.
(3) Zaia, J. *Mass Spectrom. Rev.* **2004**, *23*, 161−227.
(4) Zhou, Z.; Ogden, S.; Leary, J. A. *J. Org. Chem.* **1990**, *55*, 5444−5446.
(5) Hofmeister, G. E.; Zhou, Z.; Leary, J. A. *J. Am. Chem. Soc.* **1991**, *113*, 5964−5970.
(6) Asam, M. R.; Glish, G. L. *J. Am. Soc. Mass Spectrom.* **1997**, *8*, 987−995.
(7) Reis, A.; Domingues, M. R. M.; Ferrer-Correia, A. J.; Coimbra, M. A. *Carbohydr. Polym.* **2003**, *53*, 101−107.
(8) Reis, A.; Domingues, M. R. M.; Domingues, P.; Ferrer-Correia, A. J.; Coimbra, M. A. *Carbohydr. Res.* **2003**, *338*, 1497−1505.
(9) Nunes, F. M.; Domingues, M. R.; Coimbra, M. A. *Carbohydr. Res.* **2005**, *340*, 1689−1698.
(10) Nunes, F. M.; Reis, A.; Domingues, M. R.; Coimbra, M. A. *J. Agric. Food. Chem.* **2006**, *54*, 3428−3439.
(11) van der Kerk, S. M.; Blok-tip, L.; Hoff, Av. K.; Heerma, W.; Haverkamp, J. *Int. J. Mass Spectrom. Ion Processes* **1994**, *134*, 41−45.
(12) Xue, J.; Song, L.; Khaja, S. D.; Locke, R. D.; West, C. M.; Laine, R. A.; Matta, K. L. *Rapid Commun. Mass Spectrom.* **2004**, *18*, 1947 -1955.
(13) Mendonca, S.; Cole, R. B.; Zhu, J. H.; Cai, Y.; French, A. D.; Johnson, G. P.; Laine, R. A. *J. Am. Chem. Soc. Mass Spectrom.* **2003**, *14*, 63−78.
(14) Ashline, A. D.; Singh, S.; Hanneman, A.; Reinhold, V. *Anal. Chem.* **2005**, *77*, 6250−6262.
(15) Reinold, V. N.; Reinholhd, B. B.; Chan, S. *Methods Enzymol.* **1996**, *271*, 377−402.

10.1021/ac070317i CCC: $37.00 © 2007 American Chemical Society
Published on Web 06/23/2007

their anomeric configuration, by FAB-MS/MS of octahedral complexes of $[Co^{+3}(acac)_2/disaccharides]^+$ using kinetic energy release determination,[16] by the analysis of the fragmentation of $[M - H]^-$ observed in the negative ESI-MS,[17] and by ESI-MS/MS of $[M + Cl]^-$ ions using a triple quadrupole, based on the ratio of Cl^-/non Cl^- product ions.[18] Recently, the nonreducing glucosyl disaccharides α,α-, α,*β*-, and *β*,*β*-trehalose were distinguished by MS/MS in a quadrupole time-of-flight mass spectrometer (Q-TOF), differentiated by the ratio of the relative abundance of the product ion formed by the glycosidic cleavage versus the relative abundance of the precursor ion (*m*/*z* 203 vs 365). Wavelength-tunable infrared multiple-photon dissociation mass spectrometry, obtained in a laboratory-built FTICR mass spectrometer, enabled differentiation of linkage and anomeric configuration of disaccharides.[19] In spite of all these attempts, the direct identification of the anomeric configuration by the analyses of the product ion spectra obtained under collision-induced dissociation of the underivatized reducing disaccharide has not yet been demonstrated.[20]

Evaluation of the anomeric configuration of the oligosaccharides is a relevant issue since oligosaccharides with the same sugar composition but different anomeric configuration show distinct properties. The classical example is amylose and cellulose, two polysaccharides with very dissimilar behavior and biological functions that are composed, respectively, by maltose repeating units, α-(1→4)-glucosyl-glucose, and cellobiose repeating units, *β*-(1→4)-glucosyl-glucose. Furthermore, these two disaccharides also show distinct physical and chemical features. For example, maltose is sweet, easily digested by humans, and fermented by yeast, while cellobiose has virtually no taste, is indigestible by humans, and is not usually fermented by yeast. Many other examples can be found in nature reflecting this issue. Usually the identification of the anomeric configuration is achieved by NMR spectroscopy, which has the inconvenience of requiring large amounts of pure samples, often a very hard task considering the biological origin, diversity, and heterogeneity of most of the carbohydrates.

Enclosed in an ongoing project focused on gas-phase fragmentation of oligosaccharides from different origins under ESI-MS/MS conditions, the fragmentation patterns of the $[M + Li]^+$ ions of reducing disaccharides of glucose (Chart 1), using quadrupole time-of-flight (Q-TOF 2), linear ion trap (LIT), and triple quadrupole (QqQ) mass spectrometers, were studied. This study aimed the investigation of the possibility of disaccharide anomeric identification using mass spectrometry.

EXPERIMENTAL SECTION

The disaccharides isomaltose, cellobiose, sophorose, and kojibiose were acquired from Sigma-Aldrich (Madrid, Spain), laminaribiose was from Megazyme (Wicklow, Ireland), maltose from Riedel (Buchs, Switzerland), gentiobiose from Fluka (Buchs, Switzerland), and nigerose from Hayashibara (Okayama, Japan). Solvents used were HPLC grade.

Chart 1. Reducing Glucopyranosyl-glucose Disaccharides

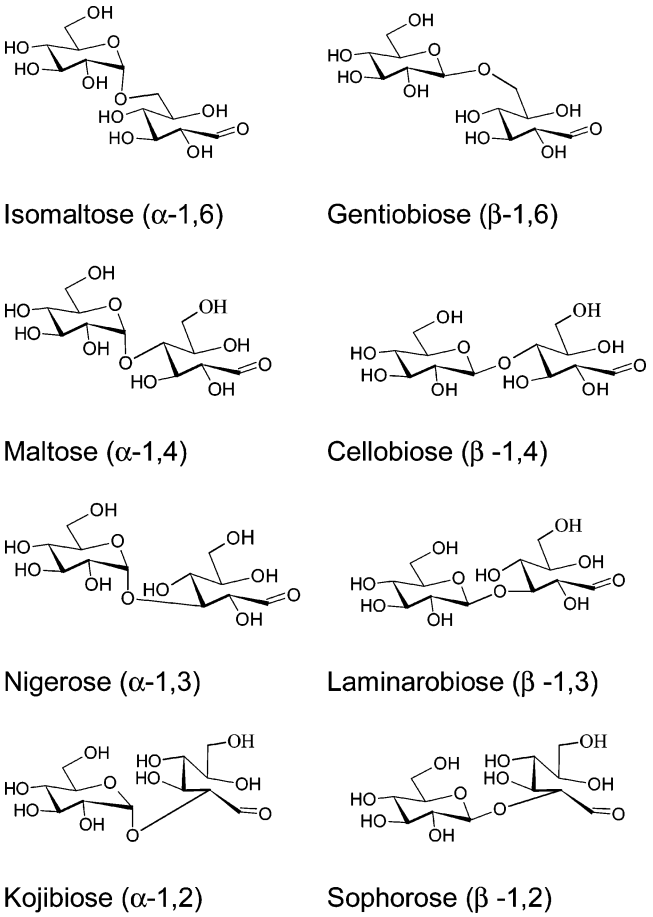

The ESI-MS and ESI-MS/MS were carried out on a Q-TOF 2 instrument (Micromass, Manchester, UK), triple quadrupole Quattro (Micromass), and a linear ion trap LXQ (ThermoFinnigan, San Jose, CA).

MS Conditions. Q-TOF. In MS and MS/MS experiments, TOF resolution was set to ~10 000 (fwhm). Samples were introduced into the electrospray source at a flow rate of 10 μL/min. The cone voltage was set at 35 V and capillary voltage at 3 kV. Source temperature was at 80 °C and desolvation temperature at 150 °C. Tandem mass spectra (MS/MS) were obtained by collision-induced decomposition (CID), using argon as the collision gas (measured pressure in the Penning gauge ~6×10^{-5} mbar). The collision energies used for lithium adducts were 25, 30, and 33 eV. Data acquisition was carried out with a MassLynx 4 data system.

Linear Ion Trap. Samples were introduced into the mass spectrometer at 10 μL min^{-1}. Typical ESI conditions were as follows: nitrogen sheath gas 30 psi, spray voltage 5,5 kV, heated capillary temperature 350 °C, capillary voltage 1 V, and tube lens voltage 40 V. CID-MS/MS experiments were performed on mass-selected precursor ions using standard isolation and excitation procedures (activation *q* value of 0.25, activation time of 30 ms). The collision energies used were 20, 22, and 24 (arbitrary units).Data acquisition was carried out with Xcalibur data system.

Triple Quadrupole. Samples were introduced into the electrospray source at a flow rate of 10 μL/min. The cone voltage was set at 35 V and capillary voltage at 3 kV. Source temperature

(16) Smith, G.; Leary, J. A. *J. Am. Soc. Mass Spectrom.* **1996**, *7*, 953−957.
(17) Mulroney, B.; Traeger, J. C.; Stone, B. A. *J. Mass Spectrom.* **1995**, *30*, 1277−1283.
(18) Jiang, Y.; Cole, R. B. *J. Am. Soc. Mass Spectrom.* **2005**, *16*, 60−70.
(19) Yamagaki, T.; Fukui, K.; Tachibana, K. *Anal. Chem.* **2006**, *78*, 1015−1022.
(20) Polfer, N. C.; Valle, J. J; Moore, D. T.; Oomens, J.; Eyler, J. R.; Bendiak, B. *Anal. Chem.* **2006**, *78*, 670−679.

was at 80 °C and desolvation temperature at 150 °C. Tandem mass spectra were obtained using Ar as the collision gas. The gas pressure in Q2 collision cell was ~1.4×10^{-3} mbar. The collision energies used for lithium adducts were 25, 30, and 33 eV. Data acquisition was carried out with a MassLynx 4 data system.

For the analysis of the lithium adducts, 5 μL of disaccharide stock solution was added to 2 μL of lithium acetate (10 mg/mL) and further diluted with water/methanol/formic acid (50/49/1, v/v/v) to a final volume of 200 μL (60 nM).

In order to simulate real sample analysis, each sample was injected in triplicate and on different days, for each instrument and collision energy. The 96 resulting mass spectra were converted into numeric tables (ion relative abundance in relation to the base peak), one for each instrument, and ions with a peak intensity of less than 5% of the base peak were not considered. This process resulted in the selection of seven product ions, which were considered as statistical variables.

Statistic Analysis. Statistics were computed using SPSS for Windows version 14.0 (SPSS Inc., Chicago, IL). The relative abundance of the selected product ions of α and β anomer disaccharide samples were tested for significance using a one-factorial multivariate analysis of variance (MANOVA). If an anomeric configuration effect was found, univariate F tests followed to identify those product ions that contributed significantly to the differences. Differences in the tandem mass spectra between α and β anomers of disaccharide samples acquired with different collision energies were also tested for significance with Pillai's trace multivariate test by applying in all cases a MANOVA. Tests with contrasts were subsequently performed for the collision energies that revealed a significant effect in order to identify, within each group, the product ions that relative abundance would significantly change with different collision energies.

An α level of 0.05 was accepted as a nominal level of significance. To keep the type I error at 0.05 or less, all a posteriori tests (univariate F tests and tests with contrasts) were performed at a reduced level of significance (α adjusted according to the Bonferroni procedure). Canonical discriminant analysis was subsequently performed to identify product ions that underlie anomeric group differences of disaccharides and build a diagnostic model. Finally, graphical assessment of both the type and the structure of correlation among the variables was performed with a scatterplot matrix.

RESULTS AND DISCUSSION

Fragmentation lithium adducts of reducing glucosyl-glucose disaccharides obtained in Q-TOF (Table 1), LIT (Table 5), and QqQ (Table 9) instruments were studied. In Figure 1 is shown, as an example, the product ion mass spectra of α and β anomers of (1→4)-linked glucosyl-glucose disaccharides, acquired using the different mass spectrometers. Product ion spectra of $[M + Li]^+$ ions showed the product ions attributable to B- and Y-type glycosidic cleavages, at m/z 169 and 187, cross-ring product ions, at m/z 289, 259, and 229, and loss of water, at m/z 331. The cross-ring fragmentations observed, as already reported,[5,6] were as follows: loss of $C_2H_4O_2$ (−60 Da), $C_3H_6O_3$ (−90 Da), and $C_4H_8O_8$ (−120 Da) for (1→6)-linked disaccharides; loss of $C_2H_4O_2$ (−60 Da) (and $C_4H_8O_8$ in the case of β) for (1→4)-linked disaccharides; loss of $C_3H_6O_3$ (−90 Da) for (1→3)-linked disaccharides; and loss of $C_4H_8O_8$ (−120 Da) for (1→2)-linked disaccharides. Lithium adducts are known to give the most informative oligosaccharide product ion spectra because, although similar fragmentations were observed for both sodium and lithium adducts, lithium adducts enhance fragmentation, as reported by several authors.[21−23] Subsequently, we have analyzed the acquired data in order to find if it was possible to discriminate anomeric disaccharides using mass spectrometry.

(a) Q-TOF Instrument. In order to explore the possibility of identification of anomeric configuration in disaccharides using a Q-TOF mass spectrometer, the relative abundances of the selected product ions of α and β anomers acquired using collision energies of 25, 30, and 33 eV were considered for statistical analysis. Acquired data are shown in Table 1. A MANOVA was used to determine differences in the relative abundance of the selected ions as influenced by collision energy and anomeric configuration. Pillai's trace was performed for post-hoc multiple comparisons as there was evidence that Pillai's trace is more robust than the other statistics to violations of model assumptions.[24] Pillai's trace revealed that both anomeric configuration and collision energy (CE) have influence on the combined dependent variables (relative abundances of product ions). In fact, the significance values of the anomeric configuration (F 235.794, df 7, $p < 0.001$) and CE (F 7.156, df 14, $p < 0.001$) are less than 0.05 (p value), indicating that the effects contribute to the model. Also the interaction anomeric configuration × collision energy was significant (F 235.794, df 7, $p < 0.001$); therefore, we conclude that there is an interaction effect on the combined dependent variables.

Univariate tests with contrasts were then performed to verify in which ions there was an effect of the anomeric conformation on the relative abundance of the product ions (Table 2). These tests indicate that there is an interaction effect between the anomeric conformation and the relative abundance of all the product ions ($p < 0.01$).

Furthermore, post-hoc analysis multiple comparison tests with Bonferroni correction revealed that, inside each group (α and β anomers), the relative abundances of the ions of m/z 331, 187, and 169 were significantly different, when comparing data acquired with CE of 25 and data acquired using both 30 and 33 eV ($p < 0.05$). An exception is the case of the product ion m/z 169, where the relative abundance of the α anomer, acquired with a CE of 25 eV, was only significantly different when using a CE of 33 eV. The relative abundance of the other ions was not significantly different in both anomeric configurations for the tested collision energies. Also, with the exception referred to above, there were no differences in the relative abundance of the ions acquired with CE of 30 and 33 eV.

Canonical discriminant analysis was subsequently performed to identify product ions that underlie anomeric group differences of disaccharides and build a diagnostic model applicable to real samples.

Although differentiation is achieved using all the CE used, the results show that CE of 25 eV (eigenvalue1 72.378, canonical correlation 0.993, Wilks' $\lambda 1 = 0.014$, $\chi^2 1 = 79.469$) and CE of

(21) Ngoka, L. C.; Gal, J.-F.; Lebrilla. C. B. *Anal. Chem.* **1994**, *66*, 692−698.
(22) Cancilla, M.; Penn, S. G.; Caroll, J. A.; Lebrilla, C. B. *J. Am. Chem. Soc.* **1996**, *118*, 6736−6745.
(23) Harvey, D. J. *J. Mass Spectrom.* **2000**, *35*, 1178 -1190.
(24) Olson, C. L. *J. Am. Stat Assoc.* **1974**, *69*, 348, 894−908.

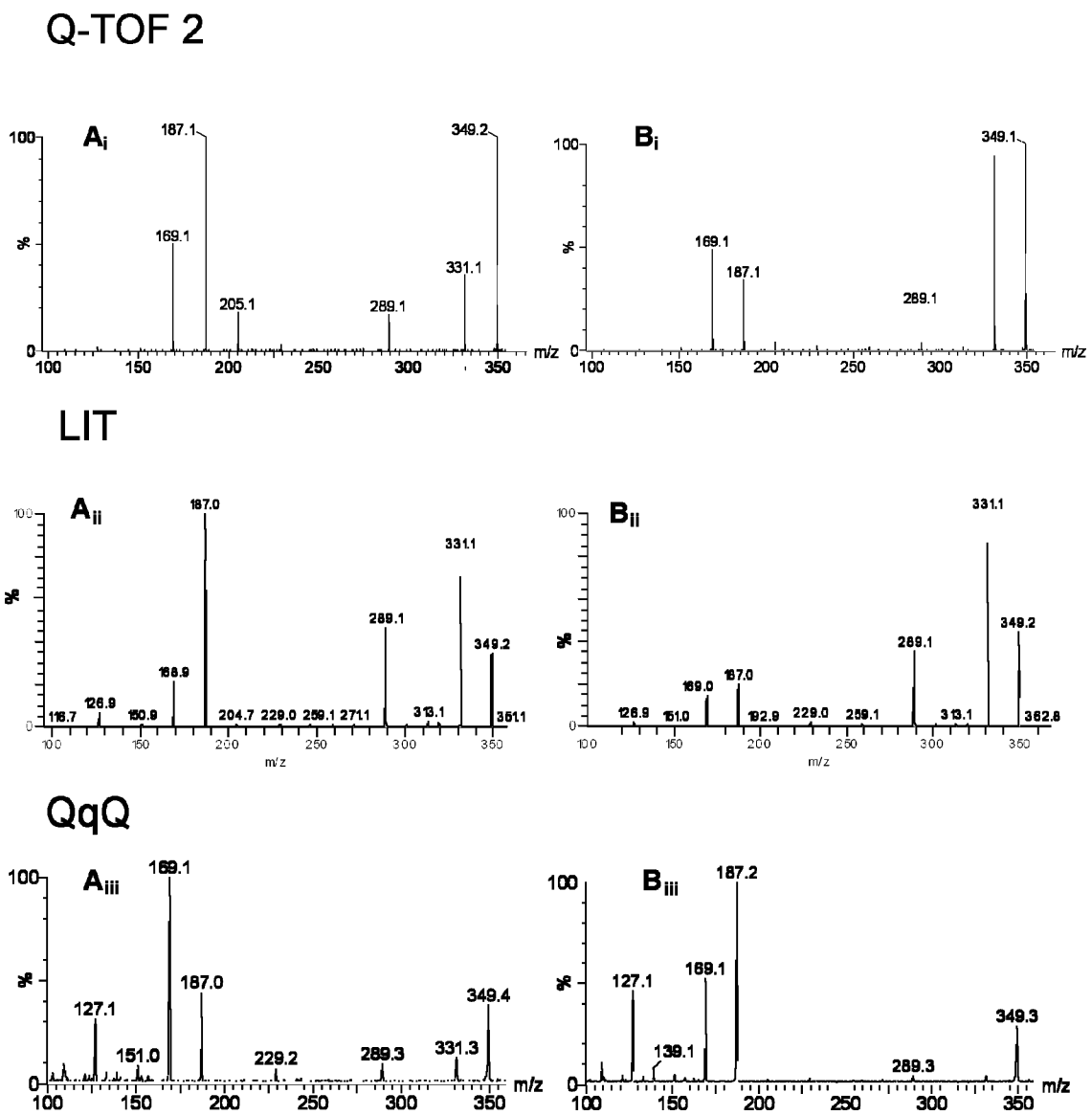

Figure 1. Product ions spectra of (A) α-(1→4) and (B) β-(1→4)-linked $[M + Li]^+$ ions, of glucopyranosyl-glucose disaccharides acquired using (i) Q-TOF 2 (CE 25 eV), (ii) LIT (CE 22), and (iii) QqQ (CE 33 eV).

33 eV (eigenvalue 64.417, canonical correlation 0.992, Wilks' $\lambda 1 = 0.015$, $\chi^2 1 = 77.34$) were the best collision energies in terms of anomeric discrimination, followed by and CE = 30 eV (eigenvalue 33.991, canonical correlation 0.986, Wilks' $\lambda 1 = 0.029$, $\chi^2 1 = 65.769$).

The discriminating function 1 (DF1) for CE of 25 eV explained 100% of the total variance with a good correlation value (0.993); therefore, we have found that this function is capable of discriminating between anomeric configuration in disaccharides using a Q-TOF mass spectrometer. A total Wilks' λ value of 0.014 ($p < 0.001$) showed a good discriminant power of the model. Wilks' λ is a statistic test used in multivariate analysis of variance to test whether there are differences between the means of identified groups of subjects on a combination of dependent variables; values of λ that are near zero denote high discrimination between groups. In Table 3, the matrix structure coefficients, showing the correlations of each variable in the model with each discriminant function are also reported. The structure coefficients are global (not partial) coefficients, similar to correlation coefficients, and reflect the uncontrolled association of the discriminating variables with the categorical variable. In Table 4, is also shown the calculated unstandardized linear discriminant coefficients, which can be used to classify cases. Each column contains estimates of the coefficients for a classification function for each group (α and β anomeric configuration). These functions are used to assign cases in the two groups. To obtain a classification score of each case in each group, multiply each coefficient by the value of the relative abundance of each ion, sum the products, and add the constant to attain the score. A case is predicted as being a member of the anomeric group in which the value of its classification function is largest. In Figure 2 is shown the projections of the observation set using the determined canonical functions.

Graphical assessment of both the type and the structure of correlation among the variables for CE = 25 eV can be accomplished by observing the scatterplot matrix on Figure 3. This scatterplot matrix illustrates the correlation of the relative abundance for every selected product ion pair within the acquired data. The matrix shows that there are several pairs of relative abun-

Table 1. Product Ions Observed in the Product Ion Spectra of the $[M + Li]^+$ Adducts of Glucopyranosyl-glucose Disaccharides Obtained in Q-TOF, Using Different Collision Energies, Showing Their *m/z* Values and the Relative Abundances

disaccharide	collision energy (eV)	product ions (*m/z*) 331	289	259	229	205	187	169
isomaltose α-1,6	25	8 ± 4	23 ± 5	12 ± 4		32 ± 13	100 ± 0	17 ± 5
	30	5 ± 1	20 ± 2	13 ± 2	7 ± 2	31 ± 17	100 ± 0	35 ± 7
	33	3 ± 2	18 ± 4	9 ± 1	8 ± 2	24 ± 14	100 ± 0	43 ± 10
maltose α-1,4	25	41 ± 4	17 ± 3			22 ± 9	100 ± 0	47 ± 7
	30	18 ± 1	11 ± 1			19 ± 7	100 ± 0	50 ± 4
	33	11 ± 3	9 ± 2			25 ± 6	100 ± 0	55 ± 2
nigerose α-1,3	25	99 ± 1		8 ± 1		13 ± 1	100 ± 1	52 ± 1
	30	22 ± 1		5 ± 0		12 ± 0	100 ± 0	61 ± 1
	33	11 ± 1		3 ± 0		13 ± 1	100 ± 0	65 ± 2
kojibiose α-1,2	25	3 ± 3			26 ± 5	26 ± 6	100 ± 0	20 ± 6
	30				21 ± 16	24 ± 8	100 ± 0	32 ± 1
	33				12 ± 3	23 ± 3	100 ± 0	38 ± 8
gentiobiose β-1,6	25	25 ± 3	100 ± 0	49 ± 3	20 ± 8	17 ± 8	57 ± 7	43 ± 9
	30	17 ± 3	100 ± 0	61 ± 6	61 ± 6	23 ± 5	89 ± 5	90 ± 3
	33	9 ± 1	72 ± 9	46 ± 8	56 ± 10	20 ± 7	84 ± 10	100 ± 0
cellobiose β-1,4	25	100 ± 0	27 ± 9		5 ± 1	8 ± 4	45 ± 10	53 ± 11
	30	78 ± 12	31 ± 1		11 ± 2	11 ± 6	63 ± 2	100 ± 0
	33	42 ± 9	22 ± 4		13 ± 5	6 ± 0	51 ± 4	100 ± 0
laminaribiose β-1,3	25	100 ± 0		9 ± 2		6 ± 1	41 ± 1	57 ± 8
	30	49 ± 2		11 ± 1		8 ± 2	68 ± 3	100 ± 0
	33	28 ± 5		8 ± 2		8 ± 2	68 ± 3	100 ± 0
sophorose β-1,2	25	3 ± 3			100 ± 0	10 ± 2	53 ± 5	23 ± 6
	30	6 ± 1			100 ± 0	16 ± 3	69 ± 11	63 ± 4
	33	4 ± 4			100 ± 0	13 ± 5	85 ± 7	78 ± 19

Table 2. *F*-Test of the Effect of Disaccharide Anomeric Configuration Using a Q-TOF Instrument[a]

dependent variable *m/z*	df	*F*	*p*	η^2	observed power[b]
331	1	8.316	0.005	0.112	0.811
289	1	9.981	0.002	0.131	0.876
259	1	8.227	0.006	0.111	0.807
229	1	20.968	0.000	0.241	0.995
205	1	24.578	0.000	0.271	0.998
187	1	294.293	0.000	0.817	1.000
169	1	91.960	0.000	0.582	1.000

[a] This test is based on the linearly independent pairwise comparisons among the estimated marginal means. [b] Computed using α = 0.05.

Table 3. Structure Matrix (Q-TOF)[a]

m/z	function 1	*m/z*	function 1
187	−0.512	169	0.039
205	−0.096	259	0.037
229	0.049	331	0.027
289	0.043		

[a] Pooled within-groups correlations between discriminating variables and standardized canonical discriminant functions. Variables were ordered by absolute size of correlation within function.

Table 4. Fisher's Linear Discriminant Functions (Q-TOF)

m/z	anomeric configuration α	β
331	0.161	0.257
289	−0.962	−0.227
259	0.102	0.066
229	−0.849	−0.017
205	−0.002	0.381
187	7.089	2.617
169	−0.641	−0.114
(constant)	−339.804	−68.424

dance of product ions (for example, product ion of *m/z* 187 with all the other product ions) that clearly discriminate between anomeric configurations.

(b) Ion Trap Instrument. Having established that discrimination between the α and β anomers was possible using a Q-TOF 2 instrument, we decided to test whether the identification of anomeric configuration in dissacharides using an ion trap mass spectrometer was also possible. For this, the relative abundances of the selected product ions of α and β anomers acquired using CE of 20, 22, and 24 (arbitrary units) were considered for statistical analysis. Acquired data is shown in Table 5. As in the previous analysis, a MANOVA was used to determine differences in the relative abundance of the selected ions as influenced by collision energy and anomeric configuration. Pillai's trace has revealed that both anomeric configuration and collision energy have influence on the combined dependent variables (relative abundances of product ions). The significance values of the anomeric configuration (*F* 158.498, df 6, $p < 0.001$) and CE (*F* 1.157, df 14, $p < 0.001$) are less than 0.05, indicating that the effects contribute to the model. The interaction anomeric configuration × collision energy was found not to be significant (*F* 0.059, df 12, $p = 1$); therefore, we conclude that in the ion trap instrument there is no interaction effect on the combined dependent variables.

Univariate tests with contrasts were then performed to verify in which product ions there was an effect of the anomeric configuration on the relative abundance of the product ions. These

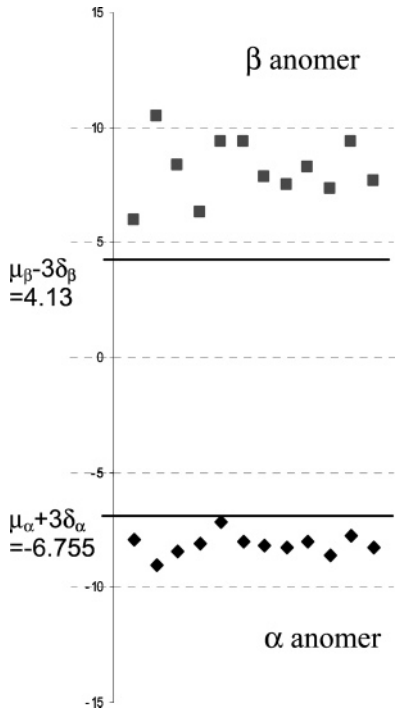

Figure 2. Discriminant analysis: projections of the observation set using the determined canonical functions. Data was acquired using a Q-TOF and a collision energy of 25 eV. μ/δ: mean value and standard deviation (α −8.15/0.465; β 8.15/1.34), *n* 24.

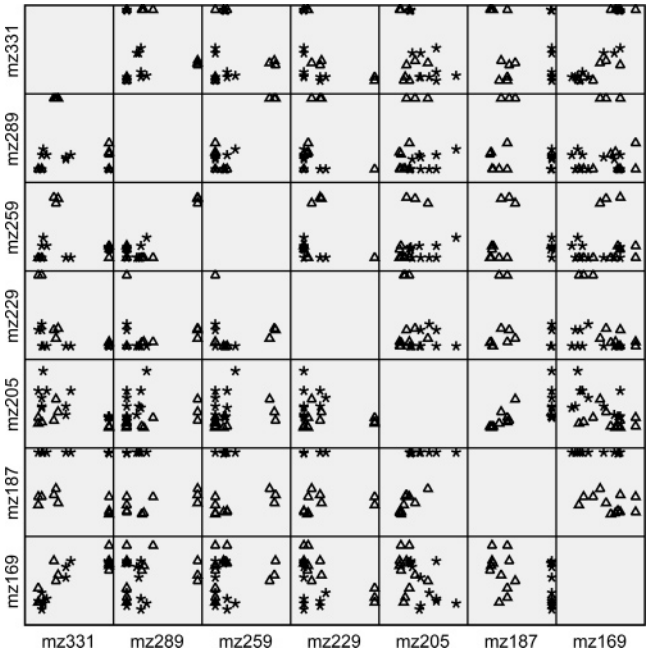

Figure 3. Scatterplot matrix for Q-TOF data acquired with CE = 25 eV. α configuration, crosses; β configuration, triangles.

tests indicate that there is an interaction effect between the anomeric configuration and the relative abundance of only the product ions m/z 187 and 169 ($p < 0.01$). As noticed, in the case of the Q-TOF instrument, there was an interaction effect with all the selected product ions.

Furthermore, post-hoc analysis multiple comparison tests with Bonferroni correction revealed that, inside each α and β anomer group, the relative abundances of the product ions were not significantly influenced by the CE ($\alpha = 0.05$).

The results of the canonical discriminant analysis subsequently performed show that CE 22 (eigenvalue1 26.119, canonical correlation 0.9813, Wilks' $\lambda 1 = 0.037$, $\chi^2 1 = 62.704$) and CE 24 (eigenvalue 24.833, canonical correlation 0.980, Wilks' $\lambda 1 = 0.039$, $\chi^2 1 = 61.781$) were the best collision energies in terms of anomeric discrimination. Although MANOVA found that the interaction anomeric configuration × collision energy was not significant, for CE = 20 (eigenvalue 12.01, canonical correlation 0.961, Wilks' $\lambda 1 = 0.077$, $\chi^2 1 = 48.749$), cross-validation analysis failed in one case.

As can be seen looking at the Wilks's λ, the discrimination power of the disaccharide anomers when using the linear ion trap instrument (CE = 22: Wilks' $\lambda 1 = 0.039$) is inferior to the Q-TOF instrument (CE of 25 eV: Wilks' $\lambda 1 = 0.014$). Also, it is important to denote that, in the case of the lower collision energy in the LIT instrument (CE = 20), there was one case incorrectly classified by the model.

Model parameters for collision energy of 22, in terms of percentage of explained variance, eigenvalues, canonical correlation values, and Wilks' λ are reported in Table 6. The DF1 explained 100% of the total variance with an acceptable correlation value (0.983); therefore, we have found that this function is able to discriminate between anomeric configurations in disaccharides using an ion trap mass spectrometer. A total Wilks' λ value of 0.037 ($p < 0.001$) showed a good discriminant power of the model. In Table 7, the matrix structure coefficients, showing the correlations of each variable in the model with each discriminant function, is also reported. As can be seen in the structure matrix, in both instruments (Q-TOF and LIT), the most discriminating ion is the product ion at m/z 187. In the case of the LIT instrument, the second most discriminating ion is the product ion at m/z 169, while in the Q-TOF instrument is the product ion at m/z 205 (Table 3). In Table 8 is also shown the calculated unstandardized linear discriminant coefficients, which can be used to classify cases. In Figure 4 is shown the projections of the observation set using the determined canonical functions.

Graphical assessment of both the type and the structure of correlation among the variables for CE = 22 can be accomplished by observing the scatterplot matrix on Figure 5. The matrix shows that discrimination of the anomer configuration by visual inspection of the mass spectra is much more difficult when using an ion trap instrument, compared with the Q-TOF. There are no pairs of relative abundance of product ions that clearly discriminate between anomeric configurations.

(c) Triple Quadrupole Instrument. In order to explore the possibility of identification of anomeric configuration in disaccharides using a QqQ mass spectrometer, the relative abundances of the selected product ions of α and β anomers acquired using CE of 25, 30, and 33 eV were considered for statistical analysis. Acquired data are shown in Table 9. MANOVA was used to determine differences in the relative abundance of the selected ions as influenced by CE and anomeric configuration. Pillai's trace revealed that both anomeric configuration and CE have influence on the combined dependent variables (relative abundances of product ions). In fact, the significance values of the anomeric configuration (F 114.025, df 6, $p < 0.001$) and CE (F 3.604, df 12, $p < 0.001$) are less than 0.05, indicating that the effects contribute to the model. As in the case of the LIT instrument, the interaction

Table 5. Product Ions Observed in the Product Ion Spectra of the [M + Li]$^+$ Adducts of Glucopyranosyl-glucose Disaccharides Obtained in LIT, Using Different Collision Energies, Showing Their *m/z* Values and the Relative Abundances

disaccharide	collision energy (au)	product ions (*m/z*) 331	289	259	229	187	169
isomaltose α-1,6	20		12 ± 5	7 ± 2	4 ± 1	100 ± 0	26 ± 3
	22		8 ± 2	5 ± 1	5 ± 2	100 ± 0	28 ± 5
	24		7 ± 3	4 ± 0	3 ± 2	100 ± 0	28 ± 8
maltose α-1,4	20	12 ± 1	8 ± 1			100 ± 0	62 ± 28
	22	6 ± 2	4 ± 1			100 ± 0	47 ± 7
	24	5 ± 1	4 ± 1			100 ± 0	46 ± 6
nigerose α-1,3	20	100 ± 0		<5		45 ± 1	45 ± 2
	22	77 ± 11		<5		95 ± 4	100 ± 0
	24	47 ± 6		<5		95 ± 5	100 ± 0
kojibiose α-1,2	20				16 ± 3	100 ± 0	17 ± 2
	22				10 ± 0	100 ± 0	20 ± 5
	24				8 ± 1	100 ± 0	22 ± 6
gentiobiose β-1,6	20	8 ± 6	53 ± 12	36 ± 15	29 ± 6	84 ± 27	89 ± 13
	22	6 ± 1	49 ± 3	31 ± 2	35 ± 5	90 ± 14	95 ± 8
	24	4 ± 0	29 ± 4	23 ± 1	31 ± 5	84 ± 14	100 ± 1
cellobiose β-1,4	20	61 ± 17	20 ± 1		6 ± 3	55 ± 2	100 ± 0
	22	28 ± 12	13 ± 2		5 ± 0	51 ± 3	100 ± 0
	24	18 ± 9	11 ± 1		6 ± 1	46 ± 6	100 ± 0
laminaribiose β-1,3	20	85 ± 26		<5		40 ± 7	99 ± 2
	22	36 ± 12		<5		41 ± 3	100 ± 0
	24	20 ± 6		<5		37 ± 3	100 ± 0
sophorose β-1,2	20				100 ± 0	74 ± 3	50 ± 6
	22				94 ± 5	96 ± 4	90 ± 17
	24				72 ± 11	82 ± 18	95 ± 9

Table 6. *F*-Test of the Effect of Disaccharides Anomeric Configuration Using a LIT Instrument[a]

dependent variable *m/z*	df	*F*	*p*	η^2	observed power[b]
331	1	.155	.695	.002	.067
289	1	.065	.800	.001	.057
259	1	.318	.575	.005	.086
229	1	.336	.564	.005	.088
187	1	130.243	.000	.664	1.000
169	1	19.305	.000	.226	.991

[a] This test is based on the linearly independent pairwise comparisons among the estimated marginal means. [b] Computed using α = 0.05.

Table 7. Structure Matrix (LIT)[a]

m/z	function 1	*m/z*	function 1
187	0.276	259	−0.012
169	0.108	331	−0.008
229	0.014	289	−0.004

[a] Pooled within-groups correlations between discriminating variables and standardized canonical discriminant functions. Variables were ordered by absolute size of correlation within function.

Table 8. Fisher's Linear Discriminant Functions (LIT)

m/z	anomeric configuration α	β
331	1.931	0.222
289	0.883	0.076
259	0.550	0.209
229	2.015	0.227
187	2.837	0.092
169	−16.496	−0.348
(constant)	−62.415	−10.532

anomeric configuration*collision energy was found not to be significant (F 0.913, df 12, $p = 0.536$); therefore, we conclude that in the QqQ instrument there is no interaction effect on the combined dependent variables.

The univariate tests with contrasts indicate that there is an interaction effect between the anomeric conformation and the relative abundance with all the product ions ($p < 0.01$), with the exception of the ion at *m/z* 331 ($p = 0.822$). These results are in more consonance with the results obtained in the Q-TOF instrument.

As in the case of the ion trap instrument, post-hoc analysis multiple comparison tests with Bonferroni correction revealed that, inside each α and β anomer group, the relative abundances of the product ions were not significantly (α = 0.05) influenced by the CE. An exception was observed for the case of the β anomers where the relative abundances of the product ions at *m/z* 331 were significantly different when acquired with CE of 25 and 33 eV ($p < 0.05$).

Canonical discriminant analysis was subsequently performed. Results show that CE 33 (eigenvalue 33.374, canonical correlation 0.985, Wilks' $\lambda 1 = 0.029$, $\chi^2 1 = 67.209$) and CE 30 (eigenvalue 32.6633, canonical correlation 0.985, Wilks' $\lambda 1 = 0.030$, $\chi^2 1 = 66.812$) were the best CE in terms of anomeric discrimination. Although MANOVA found that the interaction anomeric configuration × collision energy was not significant, for CE = 25 eV (eigenvalue1 6.433, canonical correlation 0.930, Wilks' $\lambda 1 = 0.135$, $\chi^2 1 = 38.113$), cross-validation analysis failed in one case, which means that there was one case incorrectly classified.

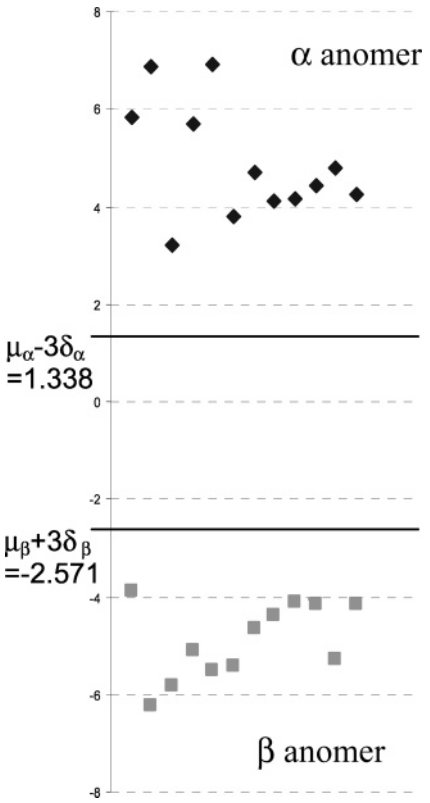

Figure 4. Discriminant analysis: projections of the observation set using the determined canonical functions. Data was acquired using a LIT and a collision energy of 22. μ/δ: mean value and standard deviation (α 4.89/1.184; β −4.89/0.773), *n* 24.

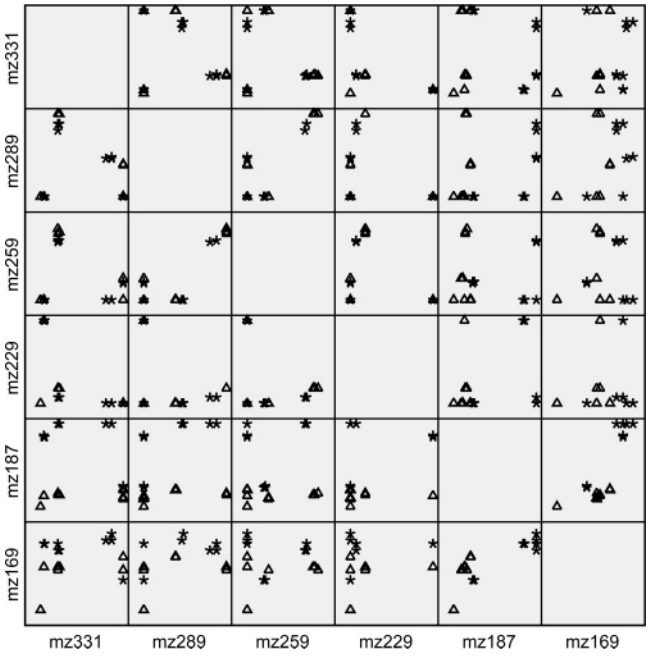

Figure 5. Scatterplot matrix for ion trap data acquired with CE = 22. α configuration, crosses; β configuration, triangles.

As can be seen looking at the Wilks' λ, the discrimination power of the disaccharide anomers when using a QqQ instrument is inferior to the Q-TOF instrument, but superior to the LIT instrument.

Model parameters for CE of 33 eV, in terms of percentage of explained variance, eigenvalues, canonical correlation values, and Wilks' λ were reported in Table 10. The DF1 explained 100% of the total variance with a good correlation value (0.985); therefore, we have found that this function is capable of discriminating between anomeric configuration in disaccharides using a QqQ mass spectrometer. A total Wilks' λ value of 0.029 ($p < 0.001$) showed a good discriminant power of the model. In Table 11, the matrix structure coefficients, showing the correlations of each variable in the model with each discriminant function, are also reported. As can be seen in the structure matrix, unlike for the Q-TOF and LIT instruments, the most discriminating ion is the product ion at *m/z* 169. The second most discriminating ion is the product ion at *m/z* 187. In Table 12 is also shown the calculated unstandardized linear discriminant coefficients, which can be used to classify cases. In Figure 6 is shown the projections of the observation set using the determined canonical functions.

Graphical assessment of both the type and the structure of correlation among the variables for CE = 33 eV can be accomplished by observing the scatterplot matrix on Figure 7. The matrix shows that there are several pairs of relative abundances of product ion at *m/z* 169 with all the other product ions that clearly discriminate between anomeric configurations.

Anomeric configuration of reducing glucosyl disaccharides was identified based on the product ion spectra of $[M + Li]^+$ ions obtained in the Q-TOF, ion trap, and triple quadrupole instruments with an electrospray source. The distinction was based on the canonical discriminant analysis. This was used to identify product ions that underlie anomeric group differences of disaccharides and build a diagnostic model applicable to real samples. MANOVA has shown that anomeric configuration has influence on the combined dependent variables (relative abundances of product ions) in the Q-TOF, LIT, and QqQ mass spectrometers used. Also, MANOVA has shown that the Q-TOF instrument is more sensitive to collision energy parameters in terms of group forming than the LIT and QqQ instruments.

Discriminant analysis has shown in all the instruments that it is possible to discriminate disaccharide anomeric configuration and to build a diagnostic model. These diagnostic differences are even more relevant considering that no derivatization procedures are needed for obtaining this structural information. Clearly this is an advantage since no manipulation of the sample is performed. Another advantage of this proposed methodology is that it can be performed in a wide variety of tandem mass spectrometers.

The Q-TOF instrument provides data that allowed us to build a model with better discriminant power (Wilks' λ value of 0.014 for CE of 25 eV) followed by the QqQ instrument (Wilks' λ value of 0.029 for CE of 33 eV) and the LIT instrument (Wilks' λ value of 0.037 for CE of 22). The number of product ions influenced by anomeric configuration is distinct from instrument to instrument. In fact, in the Q-TOF, the *F* tests of the effect of disaccharides anomeric configuration on the relative abundance of the ions has shown that all the ions are influenced, while in the LIT instrument only the ions at *m/z* 169 and 187 are influenced, and in the QqQ all except the product ion at *m/z* 331 are influenced. Other differences were seen between instruments in the order of the variables (product ion relative abundances) when ordered by absolute size of correlation within the determined function. In fact,

Table 9. Product Ions Observed in the Product Ion Spectra of the [M + Li]$^+$ Adducts of Glucopyranosyl-glucose Disaccharides Obtained in QqQ, Using Different Collision Energies, Showing their *m/z* Values and the Relative Abundances

disaccharide	collision energy (eV)	product ions (*m/z*) 331	289	259	229	187	169
isomaltose α-1,6	25	23 ± 2	83 ± 5	36 ± 3	7 ± 1	100 ± 0	19 ± 1
	30	22 ± 1	85 ± 5	36 ± 1	7 ± 0	100 ± 0	19 ± 1
	33	22 ± 1	82 ± 5	37 ± 1	8 ± 1	100 ± 0	20 ± 2
maltose α-1,4	25	83 ± 4	46 ± 2			100 ± 0	21 ± 2
	30	84 ± 4	47 ± 1			100 ± 0	22 ± 1
	33	79 ± 2	46 ± 0			100 ± 0	22 ± 1
nigerose α-1,3	25	100 ± 0		10 ± 1		23 ± 2	8 ± 1
	30	100 ± 0		11 ± 1		24 ± 1	9 ± 0
	33	100 ± 0		11 ± 1		24 ± 1	10 ± 1
kojibiose α-1,2	25	4 ± 1			100 ± 0	84 ± 2	21 ± 2
	30	4 ± 1			100 ± 0	85 ± 1	20 ± 0
	33	5 ± 1			100 ± 0	87 ± 1	21 ± 1
gentiobiose β-1,6	25	23 ± 2	100 ± 0	42 ± 2	18 ± 1	15 ± 1	13 ± 1
	30	22 ± 1	100 ± 0	41 ± 2	18 ± 0	15 ± 1	13 ± 1
	33	22 ± 1	100 ± 0	44 ± 1	19 ± 1	15 ± 1	14 ± 0
cellobiose β-1,4	25	100 ± 0	41 ± 4			20 ± 2	15 ± 1
	30	100 ± 0	39 ± 1			20 ± 1	16 ± 0
	33	100 ± 0	38 ± 1			21 ± 1	17 ± 1
laminaribiose β-1,3	25	100 ± 0		13 ± 0		9 ± 1	12 ± 1
	30	100 ± 0		13 ± 0		10 ± 1	12 ± 0
	33	100 ± 0		14 ± 1		11 ± 0	14 ± 0
sophorose β-1,2	25	4 ± 1			100 ± 0	13 ± 0	13 ± 1
	30	4 ± 0			100 ± 0	13 ± 0	13 ± 0
	33	4 ± 0			100 ± 0	13 ± 0	13 ± 0

Table 10. *F*-Test of the Effect of Disaccharides Anomeric Configuration Using a QqQ Instrument[a]

dependent variable *m/z*	df	*F*	*p*	η^2	observed power[b]
331	1	.051	.822	.001	.056
289	1	10.885	.002	.142	.902
259	1	6.434	.014	.089	.705
229	1	19.518	.000	.228	.992
187	1	40.348	.000	.379	1.000
169	1	78.520	.000	.543	1.000

[a] This test is based on the linearly independent pairwise comparisons among the estimated marginal means. [b] Computed using α = 0.05.

Table 11. Structure Matrix (QqQ)[a]

m/z	function 1	*m/z*	function 1
169	0.194	289	0.072
187	−0.191	259	0.058
229	0.103	331	−0.013

[a] Variables were ordered by absolute size of correlation within function.

Table 12. Fisher's Linear Discriminant Functions (QqQ)

m/z	anomeric configuration α	β
331	−1.231	−1.529
289	−2.656	−0.702
259	−1.033	−1.263
229	−2.357	−1.146
187	3.225	1.452
169	0.804	1.099
(constant)	−164.114	−69.357

for the Q-TOF instrument, the product ion at *m/z* 187 (−0.512) is the more discriminating ion followed by the ions at *m/z* 205 (−0.096) and 229 (0.049), while for the LIT instrument, the ion at *m/z* 187 (0.276) is the more discriminating ion followed by the ion at *m/z* 169 (0.108). For the QqQ instrument, both product ions at *m/z* 169 (0.194) and 187 (−0.191) are the more discriminating ions followed by the product ion at *m/z* 229 (0.103).

Literature about the influence of the stereospecificity of the coordination and how this can affect the collisional products both in abundance and in *m/z* is scarce. However, Cerda and Westidemiotis[25] have shown that the most stable disaccharide complexes are tetradentate and involve chair forms. Thus, small changes in the saccharide stereochemistry alter the optimum metal (Na^+) coordination and, therefore, the Na^+ affinity; thus permitting the distinction of stereoisomeric saccharides. Also, observed differences in the product ion mass spectra of disaccharide anomers may be due to the difference in energies (enthalpy) of 1−2 kcal/mol between the anomers.[26] Differences observed due to instrumental setup in the LIT and both the Q-TOF and QqQ can be rationalized due to differences in the collision cells, energies involved, and ion stability. Differences in data obtained from the Q-TOF and QqQ, which have similar collision cell geometry, may be due to differences in transmission of the product ions to the last analyzer (TOF or Q, respectively).

(25) Cerda, B. A.; Wesdemiotis, C. *Int. J. Mass Spectrom.* **1999**, *189*. 189−204.
(26) Fangmark, I.; Jansson, A.; Nilsson, B. *Anal. Chem.* **1999**, *71*, 1105−1110.

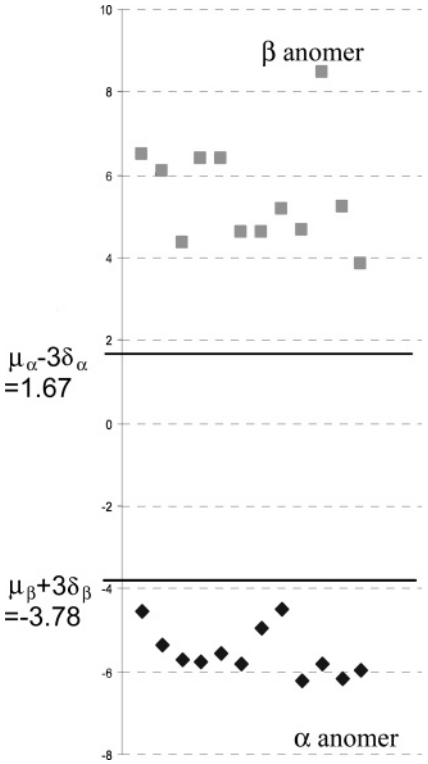

Figure 6. Discriminant analysis: projections of the observation set using the determined canonical functions. Data was acquired using a QqQ and a collision energy of 25 eV μ/δ: mean value and standard deviation (α −5.53/0.583; β 5.53/1.288), *n* 24.

CONCLUSIONS

This work successfully demonstrates that it is possible to discriminate between α and β anomers of underivatized reducing glucopyranosyl-glucose disaccharides using low-energy collisional-induced dissociation and tandem mass spectrometry in different mass spectrometers (Q-TOF, LIT, QqQ). Also, it shows that it is possible to construct for all these instruments a diagnostic model for anomeric configuration differentiation.

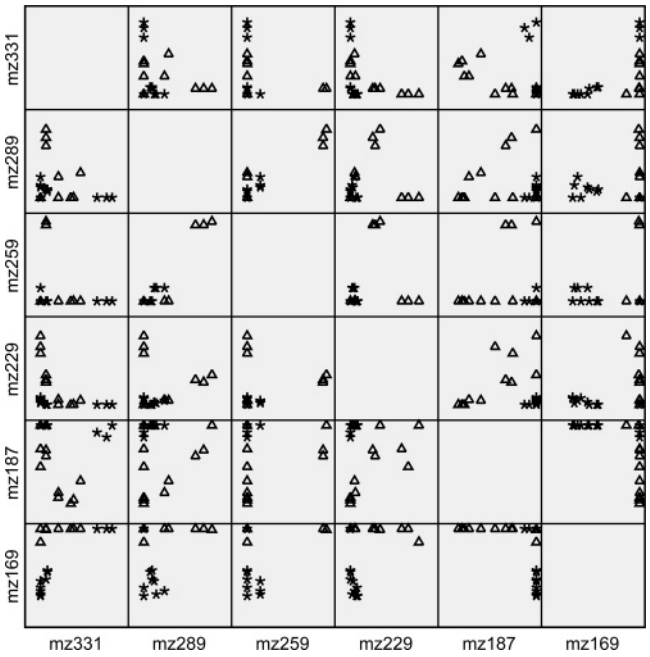

Figure 7. Scatterplot matrix for QqQ data acquired with CE = 33 eV. α configuration, crosses; β configuration, triangles.

ACKNOWLEDGMENT

The authors gratefully acknowledge the financial support provided of the project POCI/QUI/59337/2004, and Research Unit 62/94, QOPNA provided by FCT (Foundation for Science and Technology) and FEDER-FSE (III Quadro Comunitário de Apoio).

Received for review February 14, 2007. Accepted May 17, 2007.

AC070317I